PHOTOMETRIC ANALYSIS OF THE APOLLO LANDING SITES. R. N. Clegg[1] and B. L. Jolliff[1], [1]Washington University in St. Louis, Department of Earth and Planetary Sciences, 1 Brookings Drive, St. Louis, MO 63130, USA, rclegg@levee.wustl.edu

Introduction: Disturbed lunar regolith has distinctly different photometric properties than undisturbed regolith. Properties such as composition, grain size and size distribution, grain shapes, glass and Fe^0 contents, and structure (fine-scale layering or "fairy-castle" forms) determine how light is reflected from the surface [1-4]. Photometry can be used to extract this information from regions with different photometric behavior and to compare with sample analysis to improve the retrieval of information from remote sensing data [5]. Of interest here are regions around the Apollo landers that were disturbed during descent, which we refer to as blast zones. High-resolution images of the Apollo landing sites obtained by the Lunar Reconnaissance Orbiter (LRO) Narrow Angle Camera (NAC) [6] show bright regions around the Lunar Modules (LMs), which have been interpreted as disturbance of the soil due to the jets of rocket exhaust during descent of the spacecraft [7]. Our objective is to evaluate whether removal of fines, alteration of in-situ fine structure [8], exposure of less mature soil, or some other mechanism or combination of mechanisms has caused the brightness difference. We are investigating what part of the excavated particle flow regime corresponds to these areas of visible alteration using knowledge of the lunar soils from returned samples and photometric modeling.

Methods: NAC images were processed using the USGS's Integrated Software for Imagers and Spectrometers (ISIS) [9]. We use phase-ratio images (*e.g.,* Fig. 1) for each landing site to determine the size of the blast zone around each lander and to quantify the differences in reflectance within the blast zones in comparison to undisturbed regolith outside the blast zones. A phase-ratio image is made from two images of the same site with similar incidence angles (*i*) but different emission angles (*e*), and thus different phase angles (α), dividing one by the other. The two images are divided over the same pixel range to create a resultant image with high contrast between the disturbed and undisturbed soil. The new contrast ratio image allows us to distinctly see the parameters of the blast zone and infer its spatial distribution accurately.

Blast Zone Measurements: The average area of regolith brightening from measurements for the blast zones is ~29,000 m^2, with values ranging from as low as 18,800 m^2 for Apollo 15 (~150 m average diameter) to as high as 54,000 m^2 (~260 m average diameter) for Apollo 12, which has an enlarged disturbed region extending in the direction of Surveyor Crater. Most of the blast zones are elliptical in shape, but some are irregular. Our measurements indicate that the blast zones extend less than a few hundred meters from the Lunar Modules – a distance we suspect is too small to be characterized by the resettling of fines, based on particle trajectory and velocity modeling [10]. Alternatively, we are testing the hypothesis that the surface brightening in the blast zones is due to smoothing of the surface, exposure of less mature soil, and/or destruction of the fairy-castle structure of the surface layer.

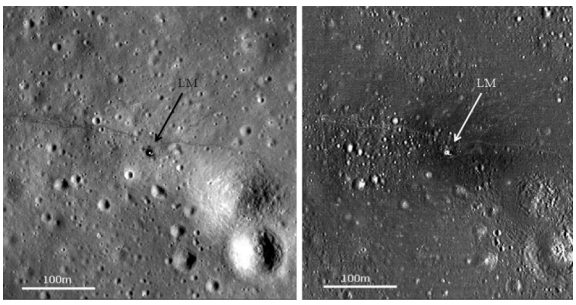

Figure 1: Ratio image for the Apollo 14 landing site compared with the NAC image. Left: NAC image, M11406206L. Right: M114064206L (*i*=57.86°, *e*=16.71°, α=41.16°) divided by M114071006L (*i*=56.94°, *e* = 22.23°, α=79.16°).

Brightness profiles were also taken across each landing site in order to help evaluate the quantitative data extracted using the phase-ratio approach. Figure 2 shows a brightness profile taken across the Apollo 11 landing site. A distinct increase in brightness is seen in the blast zone and then tapers off at distances farther from the LM, and a sharp dip in brightness is seen in the area directly around the LM. The horizontal lines indicate the average I/F values for the blast zone, under the LM, and outside the blast zone.

Photometric Analysis: For each landing site, we chose an area that encloses the blast zone, an area directly under the LM but avoiding the LM shadow, and

Table 1: Average I/F values for each Apollo landing site. Apollo 12 measurements include Surveyor Crater. Normalized I/F = (I/F_bz)/(I/F_background)

Apollo Mission	Average I/F for blast zone	Average I/F under LM	Average background I/F	Average normalized I/F
11	0.0295	0.0163	0.0262	1.132
12	0.0586	0.0542	0.0538	1.114
14	0.0553	0.0458	0.0517	1.143
15	0.0352	0.0278	0.0316	1.151
16	0.0809	0.0701	0.0760	1.069
17	0.0282	0.0256	0.0263	1.149

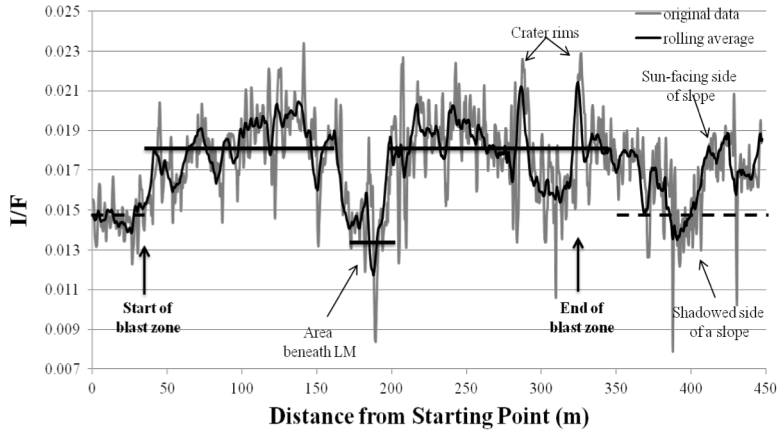

Figure 2: Profile across the Apollo 11 landing site, with solid black lines indicating average normalized reflectance within the blast zone and dashed lines showing average normalized reflectance outside the blast zone (data from bright crater rims excluded). Smoother line indicates a 10-pt. rolling average.

two areas well outside the blast zone and then record the average *i*, *e,* α, and normalized reflectance (I/F) for each region (Table 1). The average normalized reflectance is lowest for the region directly underneath the LM and greatest for the blast zone, which is in agreement with the brightness observations. The average I/F values are taken across the entire span of phase angles covered by images for each landing site. Figure 3 shows how the I/F values within the blast zone, normalized to the I/F values in the undisturbed regions, change as phase angle increases. The differences between blast zones and surrounding undisturbed regolith increases slightly as a function of phase angle.

Based on our measurements of the spatial extent of the blast zones and knowledge about the trajectory of flying particles, we suspect that excavated particle transport extended well beyond the brightened blast zone areas [10]. If so, then the higher I/F value is likely caused by some factor other than redistribution of fine particles – such as smoothing of the surface, removal of a more mature surface layer and exposure of less mature soil beneath, or a combination of effects. The area directly beneath the LM that appears darker may be explained by exposure of coarser particles, since we know that the average particle size increases with depth in lunar regolith and coarser particles experience less shadow-hiding [3]. This area could also be explained by a rougher surface because the astronauts walked around the LM and disturbed the regolith, which in turn created a darker appearance [4, 11]. A similar trend is also seen in the brightness profiles (e.g., Fig. 2), where the area beneath the LM has the lowest average I/F value.

Soils with a higher maturity are darker due to increased agglutinate content and Fe^0 content within the agglutinates [12]. Analysis of core samples also shows that the maturity decreases with depth in the top 20 cm of regolith, which should in turn create a brightening effect that should be seen if the top layer of soil is stripped off by rocket exhaust [13]. Examination of lunar samples collected both within and outside the blast zone, however, show no distinguishable trends in mean particle size and maturity differences.

Conclusions: Average I/F values are between 6 and 11% higher within the blast zones than outside. We are using photometric modeling to explore variations in soil parameters that might account for these systematic differences in reflectivity of blast zones vs. landing site backgrounds

Acknowledgements: We thank NASA for support of the LRO mission and the LROC Operations Team for the data used for this research. We thank B. Hapke and J. Plescia for helpful comments.

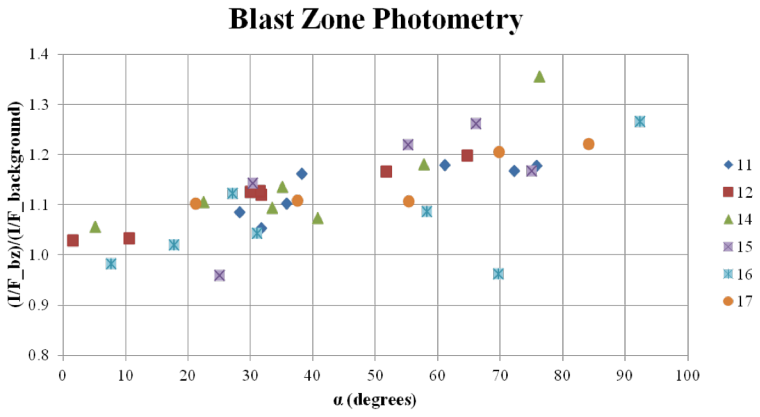

Figure 3: Photometry values as a function of phase angle within the blast zone for each landing site. Individual data points represent different NAC images.

References: [1] Carrier W.D. (1973), *The Moon, 6,* 250-263. [2] Hapke B.W. (1981), *J. Geophys. Res., 86,* 3039-3054. [3] Carrier W.D. (1991), *Lunar Sourcebook, Chpt. 9,* 475-594. [4] Kaydash V. et al. (2010), *Icarus, 211*, 89-96. [5] Goguen J.D. et al. (2010), *Icarus, 208*, 548-557. [6] Robinson M.A. et al (2010) *Space Science Reviews*, *150*, 81-124. [7] Kreslavsky M.A. and Shkuratov Y.G. (2003), *J. Geophys. Res., 108*, 5010. [8] Hapke B.W. and Van Horn H. (1963), *J. Geophys. Res., 68,* 4545. [9] Anderson J.A. et al. (2004), *LPSC XXXV*, Abstract #2039. [10] Metzger P.T. et al. (2008), *Earth and Space 2008*, 1-8. [11] Hapke, B.W. (1972), *Moon, 3,* 456-460. [12] Taylor L.A. et al. (2001), *J. Geophys. Res., 106,* 27985-27999. [13] Lucey, P. et al. (2006), *New Views of the Moon,* 84-219.